 doi:10.20944/preprints202002.0127.v1

Article

Calcium Channel Trafficking Blocker Gabapentin Bound to the $\alpha_2\delta$-1 Subunit of Voltage-Gated Calcium Channel: A Computational Structural Investigation

Wei Li *

[1] Institute of Special Environment Medicine, Nantong University, No. 9, Seyuan Road, Nantong City, Jiangsu Province, P. R. China

* Correspondence: wli148@aucklanduni.ac.nz

Received: date; Accepted: date; Published: date

Abstract: For voltage-gated Ca^{2+} channel (VGCC), its $\alpha_2\delta$ subunits are traditionally considered to be auxiliary subunits that regulates VGCC trafficking to the plasma membrane. The antiepileptic, antinociceptive and anxiolytic gabapentin (GBP) has previously been shown to bind the VGCC $\alpha_2\delta$ subunits with high affinity to disrupt VGCC trafficking. Yet, the interaction between GBP and $\alpha_2\delta$ still remains poorly understood from a structural point of view. For instance, it is not clear yet what the structural implication is of $\alpha_2\delta$-1-bound GBP against VGCC trafficking. With a set of experimental data-driven structural analysis of the VGCC $\alpha_2\delta$-1 and its ligand GBP, this article postulates for the first time that: 1), $\alpha_2\delta$-1 bound GBP stabilizes the $\alpha_2\delta$-1-GBP complex structure; 2), $\alpha_2\delta$-1 bound GBP restrains the conformational flexibility of $\alpha_2\delta$-1; 3), $\alpha_2\delta$-1-bound GBP establishes an electrostatic axis consisting of Q535 (Gln535)-R241 (Arg241)-GBP (gabapentin)-D452 (Asp452), which constitutes an energetically favourable contribution towards the structural stability of the $\alpha_2\delta$-1-GBP complex and helps restrains the conformational flexibility and local structural rigidification of $\alpha_2\delta$-1; and 4), GBP-induced local conformational inflexibility and structural rigidification of $\alpha_2\delta$-1 is one key step in the pharmacological disruption of VGCC trafficking by GBP.

Keywords: Voltage-gated calcium channel (VGCC); $\alpha_2\delta$-1 subunit; Gabapentin (GBP); Local conformational inflexibility; VGCC trafficking

1. Introduction

Voltage-gated Ca^{2+} channels (VGCCs) are important mediators of Ca^{2+} influx into electrically excitable cells [1]. Regulation of VGCCs' activity can be achieved in two principal manners: (1) direct regulation of the Ca^{2+} channel activity, and (2) the active number of channels that are embedded in the plasma membrane [1]. The molecular determinants underlying calcium channel trafficking to and from the plasma membrane is well summarized in [1]. In particular, the $\alpha_2\delta$ subunits of VGCC are traditionally considered to be auxiliary subunits that regulates VGCC trafficking to the plasma membrane [2,3] Pharmacologically, it has been established that Gabapentin (GBP) [4–8] is a ligand of the $\alpha_2\delta$ auxiliary subunits [9], and the $\alpha_2\delta$-1-bound GBP is able to disrupt VGCC trafficking [10].

GBP is a member of the antiepileptic [11,12], anxiolytic [13] and antinociceptive [14,15] drugs of the gabapentinoid family, including GBP, pregabalin and mirogabalin [4,16–23]. While the pharmacological activity of GBP is mediated by $\alpha_2\delta$ subunits, it is also prevented by site-directed mutations [24] in either $\alpha_2\delta$1 (1103 aa, GenBank accession number: O08532) or $\alpha_2\delta$2 (1156 aa, GenBank accession number: NP_001167518) that are able to abolish GBP binding, although $\alpha_2\delta$3 does not bind GBP [3,10].

Structurally, the disulfide bridge between the $\alpha_2\delta$ 1 subunit is not required for GBP binding [25]. However, α_2 alone is not able to bind GBP, suggesting that both subunits (α_2 and δ) are necessary for GBP binding [25]. Further internal deletion and site-directed (single amino acid substitution) mutagenesis study identified Arg217 of $\alpha_2\delta$-1 as critical for GBP binding [16,25]. In the meanwhile, an RRR motif just before the von Willebrand factor A (VWA) domain was found to be essential for

Preprints (www.preprints.org) | NOT PEER-REVIEWED | Posted: 10 February 2020 doi:10.20944/preprints202002.0127.v1

gabapentin binding to the $\alpha_2\delta$ 1 subunit of VGCC [24], and the third arginine in this RRR motif has been termed Arg217 (R217). Nonetheless, this numbering is taken from the end of the 24-residue signal sequence and represents Arg241 in the primary amino acid sequence of $\alpha_2\delta$-1 [3,16,17].

2. Motivation

Despite the continued development of VGCC structural biology in recent years [26–28], it still remains elusive how gabapentinoids (such as GBP or prebabalin [3,16,17,29]) exert their pharmacological activities against VGCC trafficking. Thus, with a set of experimental data-driven structural analysis of both $\alpha_2\delta$-1 and its ligand GBP, this article aims to address this question with a structural perspective.

3. Materials and Methods

As of February 9, 2020, the Protein Data Bank [30] hosts only five GBP-related experimental structures (PDB IDs: 2A1H, 2COG, 2COI, 2COJ, 2EJ3), non of which represents an experimentally determined complete (holeless [31]) complex structure of GBP-bound $\alpha_2\delta$-1. Therefore, a computational structural approach is employed here to build a complex structural model of GBP-bound $\alpha_2\delta$-1 of VGCC. The crystal structure of GBP was accessed via the Cambridge Crystallographic Data Centre (CCDC) with an access number 811428 (supplementary file **gaba.pdb**, Table 1) [32]. The structural model of $\alpha_2\delta$-1 (Table 1) was modelled using the SWISS-MODEL server (https://swissmodel.expasy.org/interactive) [33] with the Cryo-EM $Ca_V1.1$ structure (PDB ID: 6JP8) [26,27]. Afterwards, the two structures were docked using PatchDock [34] to generate 100 complex structural models, which were screened with an in-house python script (supplementary file **R241-Screen.py**, Table 1) to ensure that Arg241's side chain is in the closest spatial proximity of GBP. The screening process lead to the most outstanding 25th complex structural model (supplementary file **docking.res.25.pdb**, Table 1), which was subsequently subject to energy minimization with the YASARA server (http://www.yasara.org/minimizationserver.htm) [35] to build a complex structural model of GBP-bound $\alpha_2\delta$-1 of VGCC(supplementary file **complex.pdb**, Table 1). Afterwards, a comprehensive set of salt bridging and hydrogen bonding analysis (Table 1) was carried out as described in [36] previously.

4. Results

4.1. Building a structural model of GBP-bound $\alpha_2\delta$-1 subunit of VGCC

As described above in the Materials and Methods section, with a set of experimental data-driven structural analysis of the VGCC $\alpha_2\delta$-1 subunit and its ligand GBP, this article puts forward a set of supplementary files as outlined in Table 1, including both apo and GBP-bound $\alpha_2\delta$-1 structural models, along with the results of their salt bridging and hydrogen bonding analysis (Table 1).

Supplementary file	Notes
gaba.pdb	GBP structural model
receptor.pdb	$\alpha_2\delta$-1 structural model
receptor.pdf	Salt bridging and hydrogen bonding within $\alpha_2\delta$-1 structure
R241-Screen.py	The python script used for the screening of the GBP-bound $\alpha_2\delta$-1 structural model
docking.res.25.pdb	Output of the python script R241-Screen.py
complex.pdb	GBP-bound $\alpha_2\delta$-1 structural model
complex.pdf	Salt bridging and hydrogen bonding of the GBP-bound $\alpha_2\delta$-1 structure

Table 1. Supplementary files (with their annotations) for the potential peer review of this manuscript.

Preprints (www.preprints.org) | NOT PEER-REVIEWED | Posted: 10 February 2020 doi:10.20944/preprints202002.0127.v1

With the three-dimensional structures of both GBP (as ligand of the VGCC $\alpha_2\delta$-1 subunit, Figure 1) and $\alpha_2\delta$-1 (as receptor of GBP, Figures 2 and 3), an in silico molecular docking approach [34] was employed to construct a complex structural model of the two molecules, as shown in Figure 3.

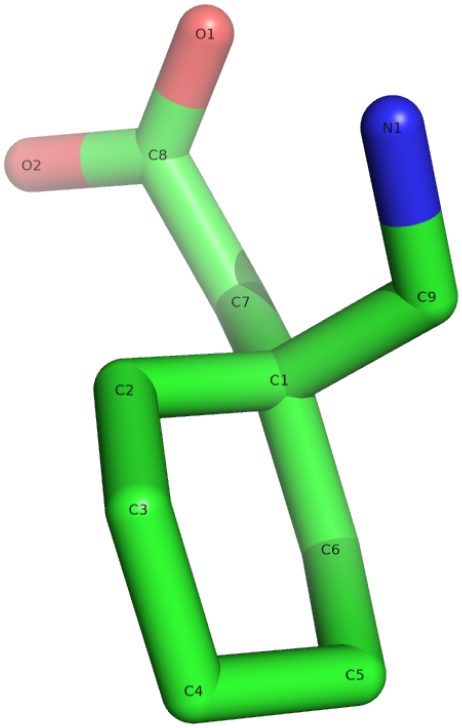

Figure 1. Crystal structure of GBP (supplementary file **gaba.pdb**, Table 1) [32]. In this figure, GBP is shown as coloured sticks, all atoms are labelled with their respective atomic symbols and numbers. This figure is prepared using PyMol [37] with gaba.pdb (Table 1) as an input.

From Figure 3, it is clear that the presence of GBP did not lead to any major conformational modification for the VGCC auxiliary $\alpha_2\delta$-1 subunit, because the two structural models of both apo and GBP-bound $\alpha_2\delta$-1 overlay quite well just with a naked-eye inspection. In further agreement with this naked-eye inspection, a quantitative analysis was carried out with supplementary file **RMSD.py** (complex.pdb and receptor.pdb (Table 1) as two inputs for this python script), yielding an RMSD value of only 1.15 Å for all backbone and side chain carbon atoms within the two structural models ((complex.pdb and receptor.pdb (Table 1)) of both apo and GBP-bound $\alpha_2\delta$-1.

To answer how exactly $\alpha_2\delta$-1-bound GBP acts against VGCC trafficking, it is necessary to really delve into the structural implication of GBP bound to the VGCC $\alpha_2\delta$-1 subunit, which is to be described below in details.

Preprints (www.preprints.org) | NOT PEER-REVIEWED | Posted: 10 February 2020 doi:10.20944/preprints202002.0127.v1

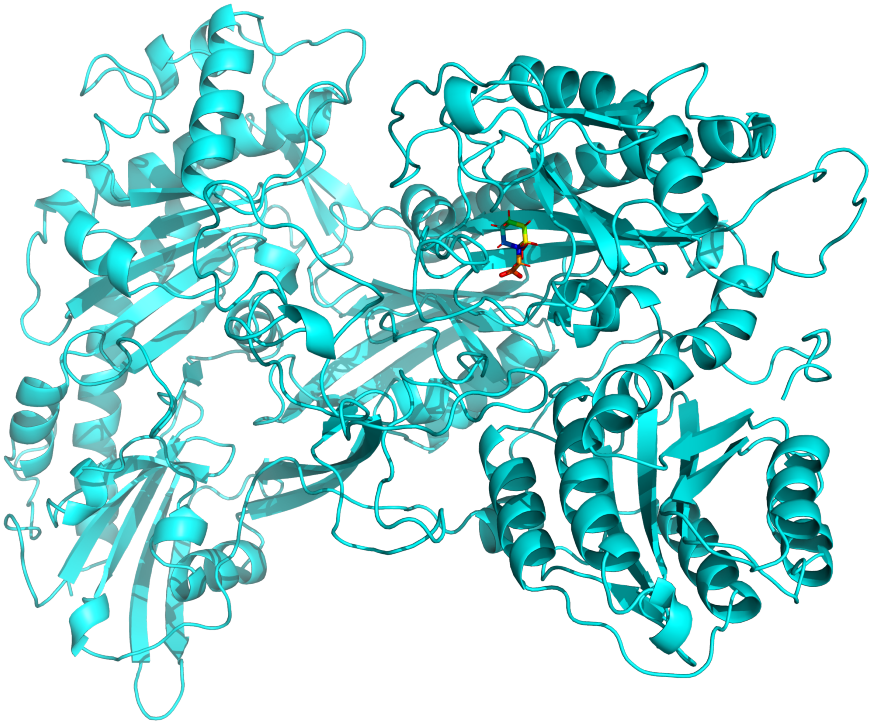

Figure 2. Structural model of GBP-bound $\alpha_2\delta$-1. In this figure, $\alpha_2\delta$-1 is shown as cyan cartoon, while GBP is shown as coloured sticks. This figure is prepared using PyMol [37] with complex.pdb (Table 1) as an input.

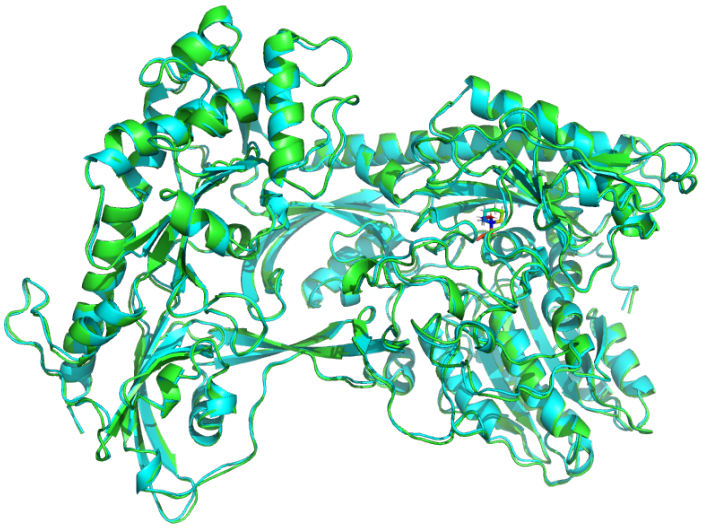

Figure 3. An overlay of the structural models of apo (green cartoon) and GBP-bound (cyan cartoon) $\alpha_2\delta$-1. In this figure, GBP is shown as coloured sticks. This figure is prepared using PyMol [37] with complex.pdb and receptor.pdb (Table 1) as two inputs.

Preprints (www.preprints.org) | NOT PEER-REVIEWED | Posted: 10 February 2020 doi:10.20944/preprints202002.0127.v1

4.2. Structural implication of GBP bound to the $\alpha_2\delta$-1 subunit of VGCC

First, a comprehensive set of structural analysis was carried out for the two structural models of both apo and GBP-bound $\alpha_2\delta$-1 as described in [36] previously, including salt bridging and hydrogen bonding analysis. The results of the structural analysis are included in two supplementary files (receptor.pdf and complex.pdf, Table 1) for the two structural models (receptor.pdf and complex.pdf, Table 1), respectively.

Nonetheless, GBP is not a typical building block of protein in that it is not classified as an amino acid chemically. As a result, an additional set of salt bridging and hydrogen bonding analysis was conducted specifically for the interaction between GBP and the VGCC $\alpha_2\delta$-1 subunit, leading to the structural identification of a GBP-induced structural axis consisting of an electrostatic quadruplet, namely Q535(Gln535)-R241(Arg241)-GBP(Gabapentin)-D452(Asp452) inside the complex structure of GBP and $\alpha_2\delta$-1, as shown in Figures 4 and 5. Specifically, the structural axis consists of GBP and an amino acid residue triplet, namely Q535(Gln535) and R241(Arg241) and D452 (Asp452), as shown in Figures 4 and 5, of the $\alpha_2\delta$-1 subunit of VGCC.

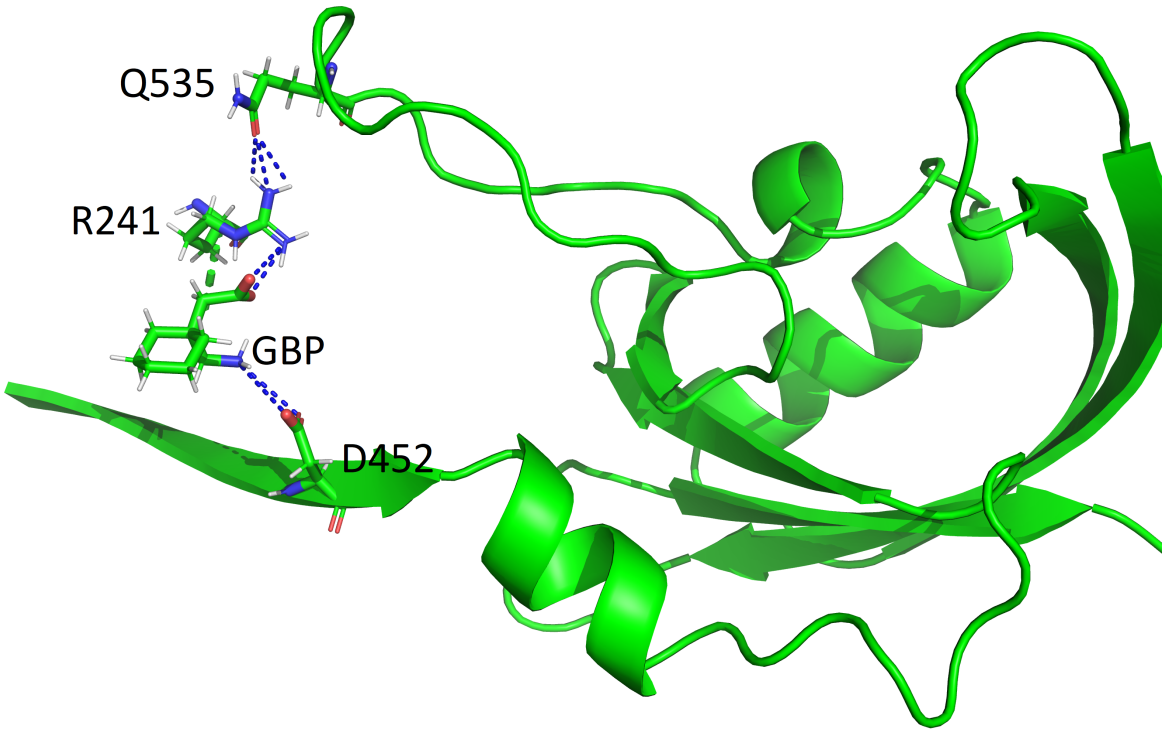

Figure 4. A GBP-induced structural electrostatic axis (Q535-R241-GBP-D452) inside the complex structure of GBP and $\alpha_2\delta$-1. This figure is prepared using PyMol [37] with complex.pdb (Table 1) as an input. In this figure, $\alpha_2\delta$-1 subunit is shown as cyan cartoon, while Gln535, R241, GBP and Asp452 are shown as coloured sticks. The structural axis Q535(Gln535)-R241(Arg241)-GBP-D452(Asp452) is stabilized by a set of electrostatic interactions between Gln535, R241, GBP and Asp452, including both salt bridges and hydrogen bonds, as shown here with a series of dotted blue lines.

As illustrated in Figures 4 and 5, the quadruplet electrostatic axis constitutes a favourable contribution towards the structural stability of the GBP-$\alpha_2\delta$-1 complex, and an unfavourable contribution towards the local conformational inflexibility of $\alpha_2\delta$-1 of VGCC, too. Specifically, the local conformational flexibility is affected for the Leu485-Thr606 motif of the VGCC $\alpha_2\delta$-1 subunit, consisting of six β-sheets, three α helices and five random coils, by the quadruplet Q535-R241-GBP-D452

Preprints (www.preprints.org) | NOT PEER-REVIEWED | Posted: 10 February 2020 doi:10.20944/preprints202002.0127.v1

electrostatic axis (Figures 4 and 5), the establishment of which is is supported by the results of the structural analysis below,

1. Q535's side chain oxygen atom is only 3.0, 3.2 and 2.8 Å away from the side chain NH_2 group of R241, as shown by Figures 6 and 7. Considering that this GBP-$\alpha_2\delta$-1 complex structure was built via a rigid-body docking approach, this article postulates that the side chains of Q535 and R241 of $\alpha_2\delta$-1 formed stable hydrogen bonds, both in the absence and in the presence of GBP.
2. R241's another side chain NH_2 group nitrogen atom is only 3.1 and 2.8 Å away from the two oxygen atoms of GBP, suggesting the existence of stable hydrogen bonds between R241's another side chain NH_2 group and the two oxygen atoms of GBP.
3. GBP's NH_2 group nitrogen atom is only 3.6 and 3.9 Å away from the side chain oxygen atoms of D452, highlighting the formation of two salt bridges between GBP and D452's negatively charged side chain.
4. No further electrostatic interaction (i.e., hydrogen bonding) was structurally identified for Q535.
5. No further electrostatic interaction was structurally identified for D452, neither salt bridging nor hydrogen bonding.

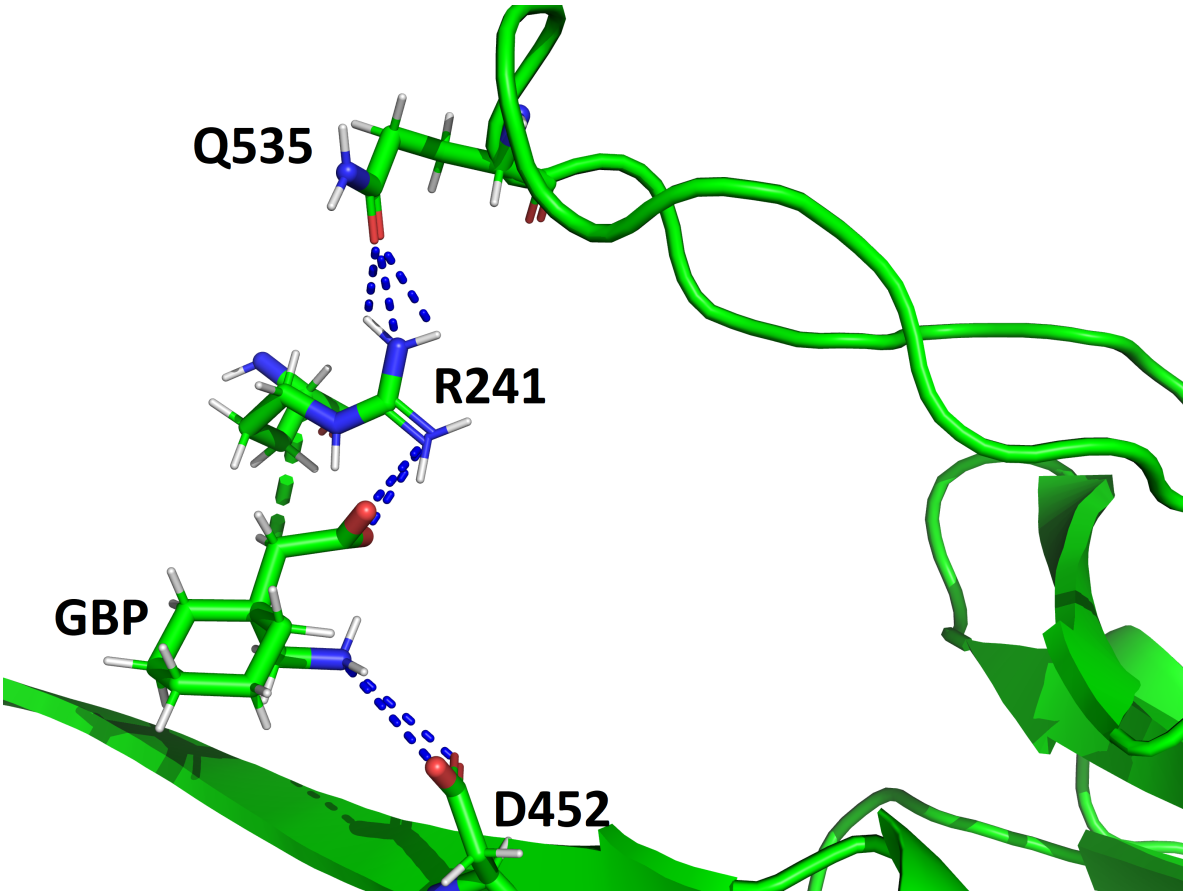

Figure 5. A closer look of the GBP-induced structural electrostatic axis (Q535-R241-GBP-D452) inside the complex structure of GBP and $\alpha_2\delta$-1. This figure is prepared using PyMol [37] with complex.pdb (Table 1) as an input. In this figure, $\alpha_2\delta$-1 is shown as cyan cartoon, while Gln535, R241, GBP and Asp452 are shown as coloured sticks. The structural axis Q535(Gln535)-R241(Arg241)-GBP-D452(Asp452) is stabilized by a set of electrostatic interactions between Gln535, R241, GBP and Asp452, including both salt bridges and hydrogen bonds, as shown here with a series of dotted blue lines.

Preprints (www.preprints.org) | NOT PEER-REVIEWED | Posted: 10 February 2020 doi:10.20944/preprints202002.0127.v1

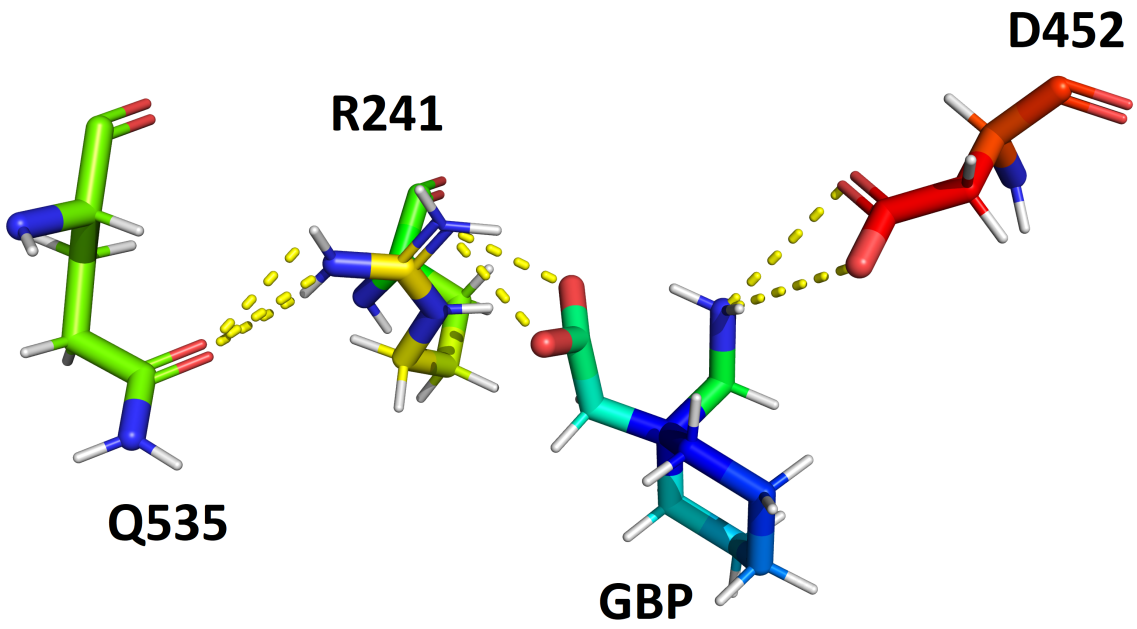

Figure 6. A GBP-induced structural axis (Q535-R241-GBP-D452) inside the complex structure of GBP and $\alpha_2\delta$-1. This figure is prepared using PyMol [37] with complex.pdb (Table 1) as an input. In this figure, $\alpha_2\delta$-1 is shown as cyan cartoon, while Gln535, R241, GBP and Asp452 are shown as coloured sticks. The structural axis Q535(Gln535)-R241(Arg241)-GBP-D452(Asp452) is stabilized by a set of electrostatic interactions between Gln535, R241, GBP and Asp452, including both salt bridges and hydrogen bonds, as shown here with a series of dotted yellow lines.

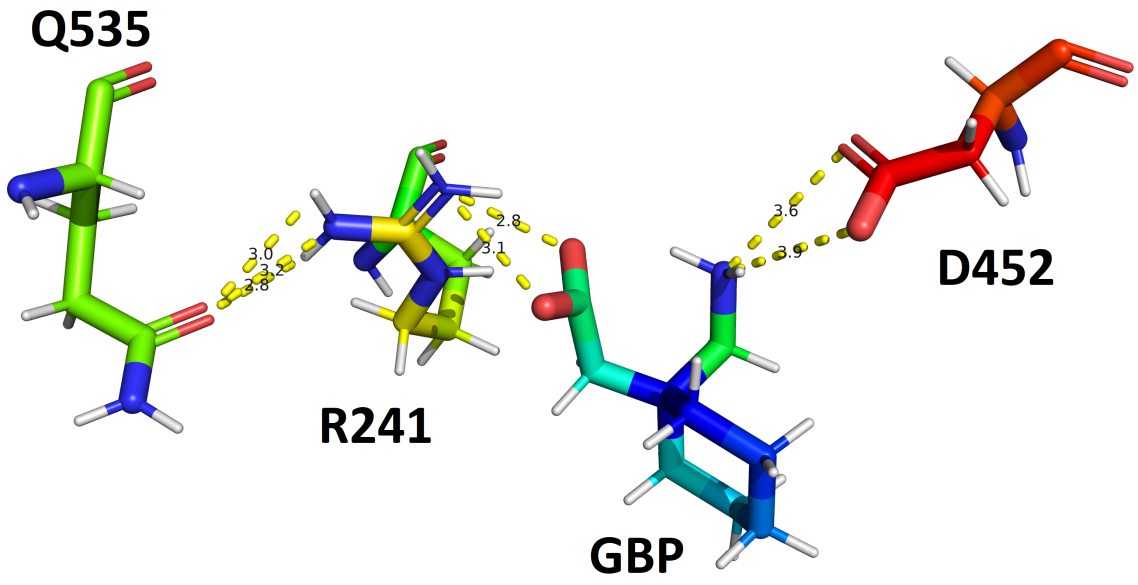

Figure 7. A GBP-induced structural axis (Q535-R241-GBP-D452) inside the complex structure of GBP and $\alpha_2\delta$-1. This figure is prepared using PyMol [37] with complex.pdb (Table 1) as an input. In this figure, $\alpha_2\delta$-1 is shown as cyan cartoon, while Gln535, R241, GBP and Asp452 are shown as coloured sticks. The structural axis Q535(Gln535)-R241(Arg241)-GBP-D452(Asp452) is stabilized by a set of electrostatic interactions between Gln535, R241, GBP and Asp452, including both salt bridges and hydrogen bonds, as shown here with a series of dotted yellow lines, the numbers (in black) nearby represent the inter-atomic distances in Å.

Preprints (www.preprints.org) | NOT PEER-REVIEWED | Posted: 10 February 2020 doi:10.20944/preprints202002.0127.v1

5. Postulation and Hypothesis

With a set of experimental data-driven structural analysis of the VGCC $\alpha_2\delta$-1 and its ligand GBP, this article postulates for the first time that,

1. $\alpha_2\delta$-1 bound GBP stabilizes the $\alpha_2\delta$-1-GBP complex structure via the quadruplet electrostatic axis, as shown by Figures 4 and 5.
2. $\alpha_2\delta$-1 bound GBP restrains the conformational flexibility of $\alpha_2\delta$-1 of VGCC via the quadruplet electrostatic axis, as shown by Figures 4 and 5.

Overall, VGCC trafficking is a complicated transmembrane process. For instance, whether the $\alpha_2\delta$ subunit undergoes major conformational movement to facilitate VGCC trafficking, is still not clear yet. Nor is it experimentally observed that GBP does disrupt VGCC trafficking via the establishment of the quadruplet electrostatic axis (Figures 4 and 5) with its $\alpha_2\delta$-1 subunit. Nevertheless, with the structural analysis and discussion above, this article for the first time puts forward two hypothesis as below,

1. Major conformational movement of the $\alpha_2\delta$ subunit, especially of the Leu485-Thr606 motif, is necessary for VGCC trafficking.
2. GBP-induced local conformational inflexibility and structural rigidification of $\alpha_2\delta$-1 is one important step in the pharmacological disruption of VGCC trafficking by GBP.

With respect to how VGCC trafficking takes place, and how VGCC trafficking blockers exert their pharmacological activities, this article calls for further investigations, both experimental and computational [28,38].

Author Contributions: Conceptualization, W.L.; methodology, W.L.; software, W.L.; validation, W.L.; formal analysis, W.L.; investigation, W.L.; resources, W.L.; data duration, W.L.; writing–original draft preparation, W.L.; writing–review and editing, W.L.; visualization, W.L.; supervision, W.L.; project administration, W.L.; funding acquisition, not applicable.

Funding: This research received no external funding.

Conflicts of Interest: The author declares no conflict of interest.

1. Simms, B.A.; Zamponi, G.W. Trafficking and stability of voltage-gated calcium channels. *Cellular and Molecular Life Sciences* **2011**, *69*, 843–856.
2. Weiss, N.; Zamponi, G.W. Trafficking of neuronal calcium channels. *Neuronal Signaling* **2017**, *1*, NS20160003.
3. Dolphin, A.C. Calcium channel auxiliary α2δ and β subunits: trafficking and one step beyond. *Nature Reviews Neuroscience* **2012**, *13*, 542–555.
4. SILLS, G. The mechanisms of action of gabapentin and pregabalin. *Current Opinion in Pharmacology* **2006**, *6*, 108–113.
5. Kelly, K. Gabapentin. *Neuropsychobiology* **1998**, *38*, 139–144.
6. Dougherty, J.A.; Rhoney, D.H. Gabapentin: A unique anti-epileptic agent. *Neurological Research* **2001**, *23*, 821–829.
7. McLean, M.J. Gabapentin. *Epilepsia* **1995**, *36*, S73–S86.
8. Beghi, E. Efficacy and tolerability of the new antiepileptic drugs: comparison of two recent guidelines. *The Lancet Neurology* **2004**, *3*, 618–621.
9. Cheng, X.; Liu, J.; Asuncion-Chin, M.; Blaskova, E.; Bannister, J.P.; Dopico, A.M.; Jaggar, J.H. A Novel CaV1.2 N Terminus Expressed in Smooth Muscle Cells of Resistance Size Arteries Modifies Channel Regulation by Auxiliary Subunits. *Journal of Biological Chemistry* **2007**, *282*, 29211–29221.
10. Hendrich, J.; Minh, A.T.V.; Heblich, F.; Nieto-Rostro, M.; Watschinger, K.; Striessnig, J.; Wratten, J.; Davies, A.; Dolphin, A.C. Pharmacological disruption of calcium channel trafficking by the α2δ ligand gabapentin. *Proceedings of the National Academy of Sciences* **2008**, *105*, 3628–3633.

11. Barclay, J.; Balaguero, N.; Mione, M.; Ackerman, S.L.; Letts, V.A.; Brodbeck, J.; Canti, C.; Meir, A.; Page, K.M.; Kusumi, K.; Perez-Reyes, E.; Lander, E.S.; Frankel, W.N.; Gardiner, R.M.; Dolphin, A.C.; Rees, M. Ducky Mouse Phenotype of Epilepsy and Ataxia Is Associated with Mutations in the *Cacna2d2* Gene and Decreased Calcium Channel Current in Cerebellar Purkinje Cells. *The Journal of Neuroscience* **2001**, *21*, 6095–6104.
12. Ivanov, S.V.; Ward, J.M.; Tessarollo, L.; McAreavey, D.; Sachdev, V.; Fananapazir, L.; Banks, M.K.; Morris, N.; Djurickovic, D.; Devor-Henneman, D.E.; Wei, M.H.; Alvord, G.W.; Gao, B.; Richardson, J.A.; Minna, J.D.; Rogawski, M.A.; Lerman, M.I. Cerebellar Ataxia, Seizures, Premature Death, and Cardiac Abnormalities in Mice with Targeted Disruption of the Cacna2d2 Gene. *The American Journal of Pathology* **2004**, *165*, 1007–1018.
13. Lotarski, S.M.; Donevan, S.; El-Kattan, A.; Osgood, S.; Poe, J.; Taylor, C.P.; Offord, J. Anxiolytic-Like Activity of Pregabalin in the Vogel Conflict Test in 2 -1 (R217A) and 2 -2 (R279A) Mouse Mutants. *Journal of Pharmacology and Experimental Therapeutics* **2011**, *338*, 615–621.
14. Field, M.J.; Cox, P.J.; Stott, E.; Melrose, H.; Offord, J.; Su, T.Z.; Bramwell, S.; Corradini, L.; England, S.; Winks, J.; Kinloch, R.A.; Hendrich, J.; Dolphin, A.C.; Webb, T.; Williams, D. Identification of the α2δ-1 subunit of voltage-dependent calcium channels as a molecular target for pain mediating the analgesic actions of pregabalin. *Proceedings of the National Academy of Sciences* **2006**, *103*, 17537–17542.
15. Publisher, B.S.P.B.S. Pharmacological Inhibition of Voltage-gated Ca^{2+} Channels for Chronic Pain Relief. *Current Neuropharmacology* **2013**, *11*, 606–620.
16. Belliotti, T.R.; Capiris, T.; Ekhato, I.V.; Kinsora, J.J.; Field, M.J.; Heffner, T.G.; Meltzer, L.T.; Schwarz, J.B.; Taylor, C.P.; Thorpe, A.J.; Vartanian, M.G.; Wise, L.D.; Zhi-Su, T.; Weber, M.L.; Wustrow, D.J. Structure-Activity Relationships of Pregabalin and Analogues That Target the α2-δ Protein. *Journal of Medicinal Chemistry* **2005**, *48*, 2294–2307.
17. Taylor, C.P.; Gee, N.S.; Su, T.Z.; Kocsis, J.D.; Welty, D.F.; Brown, J.P.; Dooley, D.J.; Boden, P.; Singh, L. A summary of mechanistic hypotheses of gabapentin pharmacology. *Epilepsy Research* **1998**, *29*, 233–249.
18. Evoy, K.E.; Morrison, M.D.; Saklad, S.R. Abuse and Misuse of Pregabalin and Gabapentin. *Drugs* **2017**, *77*, 403–426.
19. dan Li, X.; Han, C.; li Yu, W. Is gabapentin effective and safe in open hysterectomy? A PRISMA compliant meta-analysis of randomized controlled trials. *Journal of Clinical Anesthesia* **2017**, *41*, 76–83.
20. Rai, A.S.; Khan, J.S.; Dhaliwal, J.; Busse, J.W.; Choi, S.; Devereaux, P.; Clarke, H. Preoperative pregabalin or gabapentin for acute and chronic postoperative pain among patients undergoing breast cancer surgery: A systematic review and meta-analysis of randomized controlled trials. *Journal of Plastic, Reconstructive & Aesthetic Surgery* **2017**, *70*, 1317–1328.
21. Bonnet, U.; Scherbaum, N. How addictive are gabapentin and pregabalin? A systematic review. *European Neuropsychopharmacology* **2017**, *27*, 1185–1215.
22. Senderovich, H.; Jeyapragasan, G. Is there a role for combined use of gabapentin and pregabalin in pain control? Too good to be true? *Current Medical Research and Opinion* **2017**, *34*, 677–682.
23. Saeki, K.; ichi Yasuda, S.; Kato, M.; Kano, M.; Domon, Y.; Arakawa, N.; Kitano, Y. Analgesic effects of mirogabalin, a novel ligand for α2δ subunit of voltage-gated calcium channels, in experimental animal models of fibromyalgia. *Naunyn-Schmiedeberg's Archives of Pharmacology* **2019**, *392*, 723–728.
24. Brown, J.P.; Gee, N.S. Cloning and Deletion Mutagenesis of the α2δ Calcium Channel Subunit from Porcine Cerebral Cortex. *Journal of Biological Chemistry* **1998**, *273*, 25458–25465.
25. WANG, M.; OFFORD, J.; OXENDER, D.L.; SU, T.Z. Structural requirement of the calcium-channel subunit α2δ for gabapentin binding. *Biochemical Journal* **1999**, *342*, 313–320.
26. Wu, J.; Yan, Z.; Li, Z.; Qian, X.; Lu, S.; Dong, M.; Zhou, Q.; Yan, N. Structure of the voltage-gated calcium channel Cav1.1 at 3.6 Å resolution. *Nature* **2016**, *537*, 191–196.
27. Zhao, Y.; Huang, G.; Wu, J.; Wu, Q.; Gao, S.; Yan, Z.; Lei, J.; Yan, N. Molecular Basis for Ligand Modulation of a Mammalian Voltage-Gated Ca^{2+} Channel. *Cell* **2019**, *177*, 1495–1506.e12.
28. Li, W.; Shi, G. How $Ca_V1.2$-bound verapamil blocks Ca^{2+} influx into cardiomyocyte: Atomic level views. *Pharmacological Research* **2019**, *139*, 153–157.
29. Dolphin, A.C. The α2δ subunits of voltage-gated calcium channels. *Biochimica et Biophysica Acta (BBA) - Biomembranes* **2013**, *1828*, 1541–1549.

 doi:10.20944/preprints202002.0127.v1

30. Berman, H.; Henrick, K.; Nakamura, H. Announcing the worldwide Protein Data Bank. *Nature Structural & Molecular Biology* **2003**, *10*, 980–980.
31. Li, W. Visualising the Experimentally Uncharted Territories of Membrane Protein Structures inside Protein Data Bank **2020**.
32. De Vries, E.; Gamble, C.; Shaikjee, A. CCDC 811428: Experimental Crystal Structure Determination, 2011.
33. Waterhouse, A.; Bertoni, M.; Bienert, S.; Studer, G.; Tauriello, G.; Gumienny, R.; Heer, F.T.; de Beer, T.A.P.; Rempfer, C.; Bordoli, L.; Lepore, R.; Schwede, T. SWISS-MODEL: homology modelling of protein structures and complexes. *Nucleic Acids Research* **2018**, *46*, W296–W303.
34. Schneidman-Duhovny, D.; Inbar, Y.; Nussinov, R.; Wolfson, H.J. PatchDock and SymmDock: servers for rigid and symmetric docking. *Nucleic Acids Research* **2005**, *33*, W363–W367.
35. Krieger, E.; Joo, K.; Lee, J.; Lee, J.; Raman, S.; Thompson, J.; Tyka, M.; Baker, D.; Karplus, K. Improving physical realism, stereochemistry, and side-chain accuracy in homology modeling: Four approaches that performed well in CASP8. *Proteins: Structure, Function, and Bioinformatics* **2009**, *77*, 114–122.
36. Li, W. How do SMA-linked mutations of *SMN1* lead to structural/functional deficiency of the SMA protein? *PLOS ONE* **2017**, *12*, e0178519.
37. DeLano, W.L. Pymol: An open-source molecular graphics tool. *CCP4 Newsletter On Protein Crystallography* **2002**, *40*, 82–92.
38. Steven, A.C.; Baumeister, W. The future is hybrid. *Journal of Structural Biology* **2008**, *163*, 186–195.